

# Effects of B doping on hydrogen desorption from Si(001) during gas-source molecular-beam epitaxy from Si<sub>2</sub>H<sub>6</sub> and B<sub>2</sub>H<sub>6</sub>

H. Kim, G. Glass, S. Y. Park, T. Spila, N. Taylor, J. R. Abelson, and J. E. Greene<sup>a)</sup>

*Department of Materials Science, the Coordinated Science Laboratory, and the Materials Research Laboratory, University of Illinois, 1101 West Springfield, Urbana, Illinois 61801*

(Received 1 August 1996; accepted for publication 9 October 1996)

Boron doping concentrations  $\geq 6 \times 10^{19} \text{ cm}^{-3}$  were found to increase Si(001) growth rates  $R_{\text{Si}}$  at low temperatures while decreasing  $R_{\text{Si}}$  at higher temperatures during gas-source molecular beam epitaxy (GS-MBE) from Si<sub>2</sub>H<sub>6</sub> and B<sub>2</sub>H<sub>6</sub>. In order to probe the mechanisms governing these effects, Si(001) samples with B coverages  $\theta_B$  ranging from  $<0.05$  to  $\approx 0.5$  ML were prepared by exposing clean Si(001)  $2 \times 1$  wafers to B<sub>2</sub>H<sub>6</sub> doses between  $2 \times 10^{17}$  and  $4 \times 10^{20} \text{ cm}^{-2}$  at 200–400 °C. The samples were then heated to 700 °C to desorb the hydrogen, cooled to 200 °C, and exposed to atomic deuterium until saturation coverage.  $D_2$  temperature programmed desorption spectra exhibit  $\beta_2$  and  $\beta_1$  peaks due to dideuteride and monodeuteride desorption at 405 and 515 °C as well as new B-induced peaks,  $\beta_2^*$  and  $\beta_1^*$ , at 330 and 470 °C. Increasing  $\theta_B$  increases the area under  $\beta_2^*$  and  $\beta_1^*$  at the expense of  $\beta_2$  and  $\beta_1$ . Moreover, the total D coverage continuously decreases from  $\approx 1.23$  ML in the absence of B to  $\approx 0.74$  ML at  $\theta_B = 0.5$  ML. We propose that the observed B-induced decrease in the Si\*-D bond strength, where Si\* represents surface Si atoms bonded to second-layer B atoms, is due to charge transfer and increased Si\* dimer strain. The Si\* to B charge transfer also deactivates Si surface dangling bonds causing the decrease in  $\theta_D$ . These results are used to explain the GS-MBE growth kinetics. © 1996 American Institute of Physics. [S0003-6951(96)00951-5]

The incorporation probability of B from B<sub>2</sub>H<sub>6</sub> in GS-MBE Si(001) has been shown to increase linearly with increasing B<sub>2</sub>H<sub>6</sub>/Si<sub>2</sub>H<sub>6</sub> flux ratios and to decrease exponentially with inverse film growth temperature.<sup>1</sup> B is incorporated into substitutional electrically active sites at concentrations  $C_B$  up to the highest values investigated in Ref. 1,  $2.5 \times 10^{19} \text{ cm}^{-3}$ , with no measurable effect on film growth rates  $R_{\text{Si}}$ . However, even higher B concentrations are of interest for the emitter regions of heterojunction bipolar transistors in order to reduce the reverse injection current.<sup>2</sup> Recently, we have found that the use of B<sub>2</sub>H<sub>6</sub>/Si<sub>2</sub>H<sub>6</sub> flux ratios corresponding to  $C_B \geq 6 \times 10^{19} \text{ cm}^{-3}$  leads to B surface segregation and an increase in  $R_{\text{Si}}$  by up to 50% in the low-temperature surface reaction limited regime while decreasing  $R_{\text{Si}}$  by a corresponding amount in the higher temperature flux-limited regime.<sup>3</sup>

In this letter, we present the initial results of experiments designed to provide insight into the mechanism by which extremely high B doping concentrations affect GS-MBE Si(001) growth rates in opposite directions at high and low growth temperatures. Specifically, temperature programmed desorption (TPD), low energy electron diffraction (LEED), and Auger electron spectroscopy (AES) were used to investigate the effects of increasing B coverage on Si surface dangling bond coverages and Si–H bond strengths. In order to suppress the background signal during TPD measurements on clean and B-doped Si surfaces, deuterium rather than hydrogen was used to probe dangling bond coverages.

The experiments were carried out in a four-chamber ultrahigh-vacuum system<sup>1,4</sup> with a base pressure of  $\approx 5 \times 10^{-11}$  Torr. The film growth chamber, which is equipped

with reflection high energy electron diffraction (RHEED) and a quadrupole mass spectrometer (QMS), is connected through a transfer chamber to an analytical station containing provisions for AES and LEED. TPD measurements were performed in a separate chamber attached to the analytical station and containing a heavily differentially pumped Extrel QMS.

The Si(001) substrates used in these experiments were  $1 \times 3 \text{ cm}^2$  plates cleaved from 0.5-mm-thick n-type ( $n = 1 - 2 \times 10^{14} \text{ cm}^{-3}$ ) wafers. The substrate cleaning procedure described in Ref. 1 yielded starting surfaces with  $2 \times 1$  RHEED patterns and sharp Kikuchi lines. No residual C or O was detected by AES. The clean substrates were then exposed to controlled fluxes of B<sub>2</sub>H<sub>6</sub> delivered through a tubular doser located 3 cm from the substrate at an angle of 45°. Hydrogen desorption, sample annealing, and deuterium exposures were carried out in the analytical chamber.  $D_2$  was delivered through a doser identical to that described above and a hot W filament in the gas stream was used to crack the gas. For TPD experiments, the sample was placed 2 mm from the 5-mm-diam hole in the skimmer cone between the mass spectrometer and analytical chambers. Samples were heated at a linear rate, typically  $2 \text{ }^\circ\text{C s}^{-1}$ , by direct current while the temperature was determined by a thermocouple calibrated using an optical pyrometer.

B<sub>2</sub>H<sub>6</sub> exposures, typically at a flux of  $2.2 \times 10^{16} \text{ cm}^{-2} \text{ s}^{-1}$ , were carried out at temperatures between 200 and 400 °C for times ranging from 5 to 30 min. The B/Si(001) samples were then heated to 700 °C for 5 min to desorb the hydrogen. LEED patterns in all cases were  $2 \times 1$ . However, the amount of diffuse scattering increased with increasing B<sub>2</sub>H<sub>6</sub> exposure temperatures and times. This is consistent with previous scanning tunneling microscopy

<sup>a)</sup>Electronic mail: jgreene@uiuc.edu

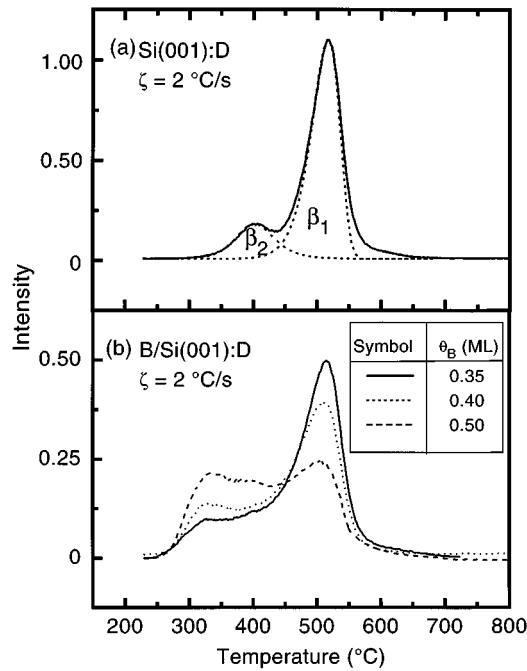


FIG. 1.  $D_2$  TPD spectra from deuterium-saturated (a) Si(001) and (b) Si(001) with preadsorbed  $B$  coverages  $\theta_B$ . The same intensity scale is used in (a) and (b).

(STM) results by Wang *et al.*<sup>5</sup> showing that B on Si(001) moves to second-layer positions and induces local ordering with  $c4 \times 4$  symmetry. The ordered domains are, however, much smaller than the LEED electron-beam coherence length so diffraction patterns remain  $2 \times 1$ . B coverages  $\theta_B$  were estimated based upon AES measurements of B KLL (178 eV) and Si LMM (92 eV) peak intensity ratios. Sensitivity factors and electron escape lengths were taken from Ref. 6 and calibration was provided using a Si(111) $\sqrt{3} \times \sqrt{3}$  test sample which was known to have 0.33 ML of  $B$  in the third layer.<sup>7</sup>  $\theta_B$  in the B/Si(001) samples ranged from less than the AES detection limit,  $\approx 0.05$  to 0.5 ML, increasing with exposure temperature in agreement with  $B_2H_6$  reactive sticking probability results in Ref. 1.

Typical  $D_2$  TPD results from a Si(001) $2 \times 1$  wafer exposed to saturation deuterium coverage, but with no  $B_2H_6$  exposure, are shown in Fig. 1(a). The spectrum consists of two peaks, labeled  $\beta_2$  and  $\beta_1$ , due to desorption from the  $1 \times 1$  dideuteride phase and the  $2 \times 1$  monodeuteride phase, respectively. The peaks are centered at 405 and 515 °C. While  $\beta_2$  desorption is second order,  $\beta_1$  follows first order kinetics, except at very low deuterium coverages  $\theta_D < 0.1$  ML,<sup>8</sup> due to  $\pi$ -bonding-induced pairing of dangling bonds on single dimers.<sup>9</sup> The data can be fit using a standard Polanyi–Wigner analysis in which the desorption rate  $d\theta_D/dT$  is expressed as<sup>10</sup>

$$\frac{d\theta_D}{dT} = - \left( \frac{\nu \theta_D^n}{\zeta} \right) \exp(-E_a/kT), \quad (1)$$

where  $\nu$  is the attempt frequency,  $\theta_D$  is the instantaneous  $D$  coverage,  $n$  is the order of the desorption reaction,  $\zeta$  is the sample heating rate,  $E_a$  is the desorption activation energy, and  $k$  is Boltzmann's constant. At high pumping speeds,<sup>11</sup>

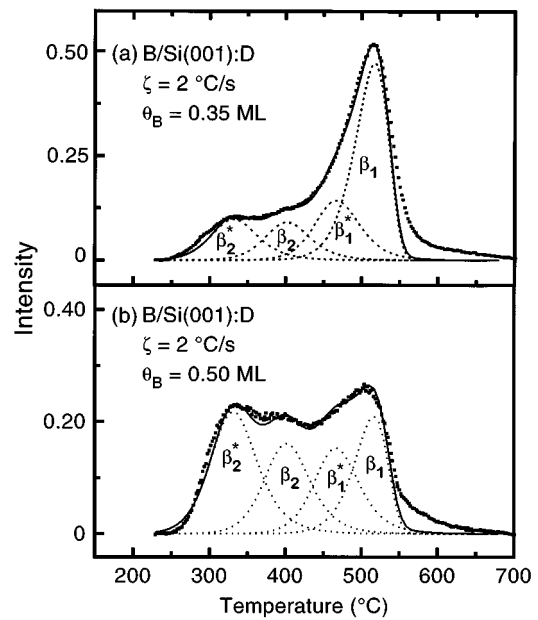


FIG. 2. Fitted  $D_2$  TPD spectra from deuterium-saturated Si(001) with preadsorbed  $B$  coverages (a)  $\theta_B = 0.35$  ML and (b)  $\theta_B = 0.50$  ML. The intensity scales are the same as in Fig. 1(a).

$$\ln \left( \frac{\theta_D(T)}{\theta_0} \right) = - \frac{\nu}{\zeta} I(T) \quad (2)$$

for first-order desorption and

$$\theta_D(T) = \frac{\theta_0}{1 + \left( \frac{\nu}{\zeta} \right) \theta_0 I(T)} \quad (3)$$

for second-order desorption.  $\theta_0$  in Eqs. (2) and (3) is the initial coverage and  $I(T)$  is given by

$$I(T) = \frac{E_a}{R} \left| \frac{e^{-\epsilon}}{\epsilon^2} \sum_{n=1}^{\infty} \frac{(-1)^{n+1} n!}{\epsilon^{n-1}} \right|_{T_0}^T \quad (4)$$

in which  $\epsilon = E_a/kT$ . The fitted results in Fig. 1(a) were obtained with  $E_a$  and  $\nu$  equal to 1.88 eV and  $1 \times 10^{13} \text{ s}^{-1}$  for  $\beta_2$  and 2.52 eV and  $1 \times 10^{15} \text{ s}^{-1}$  for  $\beta_1$  in reasonable agreement with Refs. 8 and 12. The relatively poor fit at the highest temperatures is also observed for Si(001):H TPD<sup>13</sup> and due, as noted above, to the fact that  $\beta_1$  desorption deviates from first-order kinetics at low  $D$  (or H) coverages.

Typical  $D_2$  spectra from  $B$ -doped Si(001) surfaces are shown in Fig. 1(b). Compared to the pure Si TPD spectra in Fig. 1(a) the adsorption of  $B$  has clearly reduced the onset temperature for  $D_2$  desorption while the features have broadened indicating the presence of new peaks. In addition, the total saturated  $D_2$  coverage decreases with increasing  $B$  concentration from 1.23 ML with no  $B$  exposure to 0.84, 0.82, and 0.74 ML with  $\theta_B = 0.35, 0.40,$  and  $0.50$ , respectively. This stems primarily from the rapid decrease in  $\beta_1(\theta_B)$ .

All  $D_2$  TPD spectra from  $B$  preadsorbed samples were found to be well fit with four peaks: the initial  $\beta_2$  and  $\beta_1$  peaks together with the two lower-temperature  $B$ -induced  $\beta_2^*$  and  $\beta_1^*$  peaks at 330 and 470 °C. Examples of fitted spectra are shown in Figs. 2(a) and 2(b) for samples with

$\theta_B = 0.35$  and  $0.50$  ML. Best fit values for  $E_a$  and  $\nu$  are  $1.56$  eV and  $1 \times 10^{12} \text{ s}^{-1}$  for  $\beta_2^*$  and  $2.29$  eV and  $3 \times 10^{14} \text{ s}^{-1}$  for  $\beta_1^*$ .

Previous STM results,<sup>5</sup> have show that  $B$ -induced Si(001) surface reconstructions consist of two primary  $c4 \times 4$  structural subunits containing four second-layer  $B$  atoms and two first-layer Si dimers with  $B$  backbonds. In one subunit, there is also a dimer vacancy while in the other there is an additional Si dimer which is unmodified and bonded only to second-layer Si atoms. Thus, the  $\beta_1$  and  $\beta_2$  peaks should be observed even for  $\theta_B = 0.5$  ML, in agreement with the results in Figs. 1(b) and 2(b), since undisturbed Si dimers still exist.

The Si–B bond length,  $2.0\text{--}2.1 \text{ \AA}$ ,<sup>14</sup> is considerably shorter than Si–Si,  $2.35 \text{ \AA}$ , and  $B$  has both a higher electronegativity than Si and an empty  $sp^3$  orbital. Thus, we propose that the decrease observed in  $\theta_D$  with increasing  $\theta_B$  is, in addition to the increased concentration of Si dimer vacancies, due to the partial deactivation of Si dangling bonds resulting from charge transfer from Si adatoms to subsurface  $B$  similar to the case for B/Si(111) $\sqrt{3} \times \sqrt{3}$  in which charge transfer was deduced from tunneling spectra.<sup>15</sup> The deactivation of Si dangling bonds also reduces the tendency for  $D$  atoms to pair up on single dimers and thus leads to second order  $\beta_1^*$  desorption kinetics. The lower activation energies measured for deuterium desorption from Si\*– $D$  and Si\*– $D_2$  (where Si\* signifies a  $B$ -bonded Si adatom) results from the combination of Si\*– $B$  backbond charge transfer and the additional strain in Si\* dimers.

The  $\beta_2/\beta_1$  integrated area ratio in Fig. 1(a) for non- $B$ -exposed Si(001) is  $0.23$ , far less than the value of unity which would be expected for complete dideuteride coverage. This has been explained previously for Si(001) with saturated H coverage as being due to steric hindrance resulting from electronic repulsion between adsorbed H nearest neighbors.<sup>16</sup> However, the results in Fig. 2 show that the  $\beta_2/\beta_1$  ratio increases with  $B$  coverage ( $\beta_2/\beta_1 = 0.30$  and  $0.81$  at  $\theta_B = 0.35$  and  $0.50$  ML). This is because the steric hindrance is partially removed since unmodified Si dimers have no nearest neighbors in adjacent 110 dimer rows. At  $\theta_B = 0.5$  ML, the fraction of unmodified Si dimers is approximately  $0.25$  in rough agreement with the reduction in the  $\beta_1$  peak area from that measured for pure Si(001): $D$ . A similar scaling is observed at lower  $B$  coverages.

The deposition rate during GS-MBE Si(001) from  $\text{Si}_2\text{H}_6$  is given by  $R_{\text{Si}} = 2J_{\text{Si}_2\text{H}_6} S_{\text{Si}_2\text{H}_6} \theta_{db}^2 / N$  where  $J_{\text{Si}_2\text{H}_6}$  and

$S_{\text{Si}_2\text{H}_6}$  are the incident  $\text{Si}_2\text{H}_6$  flux and reactive sticking probability,  $\theta_{db}$  is the dangling bond coverage, and  $N$  is the bulk Si atom density.<sup>17</sup> At low film growth temperatures,  $R_{\text{Si}}$  is very strongly dependent upon  $\theta_{db}$  which is a complex function of  $S_{\text{Si}_2\text{H}_6}$ ,  $J_{\text{Si}_2\text{H}_6}$ ,  $T_s$ , and the hydrogen desorption rate. Our TPD results clearly show that high subsurface  $B$  coverages result in a weakening of Si\*–H bonds, thus increasing the hydrogen desorption rate which, in turn, increases  $\theta_{db}$  in the surface reaction limited regime and, hence, increases  $R_{\text{Si}}$ . At high film growth temperatures in the absence of  $B$ ,  $\theta_{db}$  approaches unity,  $S_{\text{Si}_2\text{H}_6}$  is essentially independent of  $T_s$ , and  $R_{\text{Si}} \propto J_{\text{Si}_2\text{H}_6}$ .<sup>17</sup> Thus, in the impingement flux limited regime, the primary effect of high  $B$  coverages is to deactivate a fraction of the Si dangling bonds leading to a decrease in  $\theta_{db}$  and the observed decrease in  $R_{\text{Si}}$  at constant  $J_{\text{Si}_2\text{H}_6}$ . We have performed TPD measurements on very highly doped GS-MBE Si:B films. The spectra are similar to those shown in Figs. 1(b) and 2 and can thus be used to estimate  $B$  surface coverages.

The authors acknowledge the financial support of the Office of Naval Research through Contract Nos. NOOO 14-92-J-1649 and 14-96-0280 administered by Dr. Al Goodman.

<sup>1</sup> Q. Lu, T. R. Bramblett, N.-E. Lee, M.-A. Hasan, T. Karasawa, and J. E. Greene, *J. Appl. Phys.* **77**, 3067 (1995).

<sup>2</sup> T. P. Pearsall, *Thin Solid Films* **184**, 451 (1990).

<sup>3</sup> G. Glass, M. R. Sardela, and J. E. Greene (unpublished).

<sup>4</sup> Q. Lu, T. R. Bramblett, M.-A. Hasan, and J. E. Greene, *J. Appl. Phys.* **78**, 6027 (1995).

<sup>5</sup> Y. Wang and R. J. Hamers, *Appl. Phys. Lett.* **56**, 2057 (1995); and *J. Vac. Sci. Technol. A* **13**, 1431 (1995); Y. Wang, R. J. Hamers, and E. Kaxiras, *Phys. Rev. Lett.* **74**, 403 (1995).

<sup>6</sup> C. C. Chang, *Surf. Sci.* **48**, 9 (1975).

<sup>7</sup> P. J. Chen, M. L. Colaianni, and J. T. Yates, Jr., *J. Appl. Phys.* **72**, 3155 (1992).

<sup>8</sup> U. Höfer, L. Li, and T. F. Heinz, *Phys. Rev. B* **45**, 9485 (1992).

<sup>9</sup> J. J. Boland, *J. Vac. Sci. Technol. A* **10**, 2458 (1992).

<sup>10</sup> P. A. Redhead, *Vacuum* **12**, 203 (1962).

<sup>11</sup> F. M. Lord and J. S. Kittelberger, *Surf. Sci.* **43**, 173 (1974).

<sup>12</sup> M. C. Flowers, N. B. H. Jonathan, Y. Liu, and A. Morris, *J. Chem. Phys.* **99**, 7038 (1993); P. Gupta, V. L. Colvin, and S. M. George, *Phys. Rev. B* **37**, 8234 (1988); M. L. Wise, B. G. Kohler, P. Gupta, P. A. Coon, and S. M. George, *Surf. Sci.* **258**, 166 (1991).

<sup>13</sup> G. Boishin and L. Surnev, *Surf. Sci.* **345**, 64 (1966).

<sup>14</sup> B. E. Weir, R. L. Headrick, Q. Shen, L. C. Feldman, M. S. Hybertson, M. Needels, M. Schluter, and T. R. Hart, *Phys. Rev. B* **46**, 12 861 (1992).

<sup>15</sup> Ph. Avouris, I.-W. Lyo, F. Bozso, and E. Kaxiras, *J. Vac. Sci. Technol. A* **8**, 3405 (1990).

<sup>16</sup> J. E. Northrup, *Phys. Rev. B* **44**, 1419 (1991).

<sup>17</sup> T. R. Bramblett, Q. Lu, T. Karasawa, M.-A. Hasan, S. K. Jo, and J. E. Greene, *J. Appl. Phys.* **76**, 1884 (1994).